CDD*press*

Check for updates

ARTICLE

Genetic interaction between PLK1 and downstream MCPH proteins in the control of centrosome asymmetry and cell fate during neural progenitor division

José González-Martínez [1], Andrzej W. Cwetsch[1,2], Javier Gilabert-Juan [1,8], Jesús Gómez [3], Guillermo Garaulet[4], Paulina Schneider[1], Guillermo de Cárcer [1,9], Francisca Mulero[4], Eduardo Caleiras[5], Diego Megías[3], Eva Porlan[1,6,7] and Marcos Malumbres [1]✉

Alteration of centrosome function and dynamics results in major defects during chromosome segregation and is associated with primary autosomal microcephaly (MCPH). Despite the knowledge accumulated in the last few years, why some centrosomal defects specifically affect neural progenitors is not clear. We describe here that the centrosomal kinase PLK1 controls centrosome asymmetry and cell fate in neural progenitors during development. Gain- or loss-of-function mutations in *Plk1*, as well as deficiencies in the MCPH genes *Cdk5rap2* (*MCPH3*) and *Cep135* (*MCPH8*), lead to abnormal asymmetry in the centrosomes carrying the mother and daughter centriole in neural progenitors. However, whereas loss of MCPH proteins leads to increased centrosome asymmetry and microcephaly, deficient PLK1 activity results in reduced asymmetry and increased expansion of neural progenitors and cortical growth during mid-gestation. The combination of PLK1 and MCPH mutations results in increased microcephaly accompanied by more aggressive centrosomal and mitotic abnormalities. In addition to highlighting the delicate balance in the level and activity of centrosomal regulators, these data suggest that human *PLK1*, which maps to 16p12.1, may contribute to the neurodevelopmental defects associated with 16p11.2–p12.2 microdeletions and microduplications in children with developmental delay and dysmorphic features.

INTRODUCTION

Centrosomes are nonmembranous organelles that instruct the organization of microtubules during interphase and the mitotic spindle, thus allowing equal segregation of DNA to daughter cells [1–3]. Cumulative evidences in the last few years have established an initially surprising connection between mutations in centrosome regulators and primary autosomal microcephaly (MCPH), a disease characterized by limited expansion of the brain during development [4]. Multiple centrosome proteins, including CDK5RAP2 (encoded by *MCPH3*), ASPM (*MCPH5*), and CEP135 (*MCPH8*) (Supplementary Fig. 1a), are encoded by genes mutated in MCPH, and why neural development is especially sensitive to these mutations or to defects in centrosome structure or function is currently unclear.

At early neurodevelopmental stages, the pool of neural progenitors (NPs) is expanded by symmetric, proliferative cell divisions, whereas in later developmental stages, NPs switch to divide by asymmetric, differentiative cell divisions, giving rise to a hierarchy of differently fated cell types that generate the structural

and functional complexity of the developing neocortex [5]. The hierarchy of NPs is structured in two germinal layers: the ventricular zone (VZ), a pseudostratified neuroepithelium of apical neural progenitors (APs), and the subventricular zone (SVZ), which is populated by basal progenitors (BPs), a group of NPs that stem from the differentiative cell divisions of APs [6]. NPs eventually differentiate through several rounds of cell division to produce neurons that migrate away to populate the neocortical plate. In addition to contributing to the establishment of a bipolar mitotic spindle, centrosomes also allow interkinetic nuclear movement to promote a cell cycle-dependent pseudoestratification of NPs and the shaping of the developing central nervous system [7]. In mice, the centrosome containing the mother centriole is also key to maintain APs attached to the apical surface, and this centrosome asymmetry contributes to defining the cell fate of daughter cells after division of APs [7, 8].

Centrosome function and dynamics is a complex process controlled by structural components (such as γ-tubulin and

[1]Cell Division and Cancer group, Spanish National Cancer Research Centre (CNIO), Madrid, Spain. [2]Imagine Institute of Genetic Diseases, University of Paris, Paris, France. [3]Confocal Microscopy Core Unit, CNIO, Madrid, Spain. [4]Molecular Imaging Core Unit, CNIO, Madrid, Spain. [5]Histopathology Core Unit, CNIO, Madrid, Spain. [6]Centro de Biología Molecular "Severo Ochoa", Consejo Superior de Investigaciones Científicas-Universidad Autónoma de Madrid (CSIC-UAM), Madrid, Spain. [7]Departamento de Biología Molecular, UAM, Spain, Instituto de Investigación Hospital Universitario La Paz (IdiPAZ), Instituto de Salud Carlos III, Madrid, Spain. [8]Present address: Departamento de Anatomía, Histología y Neurociencia. Universidad Autónoma de Madrid, 28049 Madrid, Spain. [9]Present address: Instituto de Investigaciones Biomédicas (IIB-CSIC), 28029 Madrid, Spain. ✉email: malumbres@cnio.es
Edited by A. Villunger

several MCPH proteins), as well as master regulatory kinases of the Aurora and Polo families (Supplementary Fig. 1a). Polo-like kinase 1 (PLK1) is a master regulator of centrosome structure and function at least partially by regulating CDK5RAP2 (MCPH3) activity in centrosome maturation among other activities [9, 10]. Although no mutations in Aurora or PLK1-encoding genes have been found in MCPH, a cohort of pediatric patients bearing brain-size defects present a recurrent microdeletion of a pericentromeric region on chromosome 16 where the human PLK1 gene is located (16p11.2–p12.2) [11]. These patients display multiple neurodevelopmental alterations concurrent with behavioral and cardiovascular problems. However, the contribution of the multiple genes mapped to the regions involved is unclear due to the complexity of multiple rearrangements [12–17].

Whereas the involvement of structural components has been studied in multiple mouse models, the relevance of centrosomal kinases in microcephaly has been poorly explored. In this work, we compare the effects of mutations in both structural (CDK5RAP2 and CEP135) and enzymatic (PLK1) components of centrosome function in neurodevelopment, as well as their genetic interactions. By using genetically modified mouse models, we describe the relevance of proper PLK1 levels and activity in centrosome maturation, and cell fate of neural progenitors. Our observations suggest that MCPH proteins and centrosomal kinases interact in determining centrosome asymmetry and cell fate after mitotic division in neural progenitors.

RESULTS
PLK1 deregulation prevents proper neural development
We directly assessed the effect of modulating PLK1 activity during cortical development by using loss- and gain-of-function genetic models. As expected from the essential role of this kinase during mitosis [18–20], elimination of PLK1 using a conditional knockout allele [21, 22] driven by the Nestin promoter [Plk1(Δ/Δ); Nes-Cre] resulted in a dramatic phenotype in which mid-gestation embryos (E15.5) were almost completely devoid of NPs (Fig. 1a). This phenotype correlated with abundant mitotic abnormalities and loss of neural progenitors at early time points (Supplementary Fig. 1b).

On the other hand, we tested the effect of PLK1 overexpression by using a knock-in allele [tet_Plk1(T)] in which Plk1 expression is driven by tetracycline-inducible sequences and can be induced upon the addition of doxycycline (Dox) [23]. Administration of Dox to pregnant females by E12.5 resulted in strong overexpression of PLK1 in the proliferative layers of the developing neuroepithelium by E14.5, concomitant with severe microcephaly and a smaller neocortex (Fig. 1b). Whereas no changes were observed in SOX2 + VZ progenitors, PLK1 overexpression correlated with an increase in the number of cells positive for the mitotic marker phospho-histone H3 scattered in adventricular location within the neocortex (S10ph; PH3; Fig. 1b and Supplementary Fig. 1c). In addition, PLK1-overexpressing developing brains displayed a significant increase in SOX2 + cells in the intermediate layers, in most cases, negative for the mitotic marker PH3 (Fig. 1c, d and Supplementary Fig. 1c). These observations correlated with the presence of apoptotic cells (showing active caspase 3), both in the ventricular and subventricular layers (Fig. 1e). In line with these findings, PLK1-overexpressing embryos were not able to progress through late gestation, and no newborns were recovered after birth (Supplementary Fig. 1d). Collectively, these data support the notion that appropriate levels of PLK1 are required for a correct neurodevelopment in mouse embryos.

PLK1 modulates centrosomal asymmetry and cell fate in cortical NPs
To analyze the effect of partial modulation of PLK1, we next tested the effect of specific small-molecule inhibitors (iPLK1) commonly used in preclinical assays and clinical trials for cancer therapy [24]. We first titrated three different inhibitors in cultured NPs isolated from developing E14.5 cortices to select concentrations that did not induce the known mitotic defects (mostly monopolar spindles), resulting from the complete absence of PLK1 activity (Supplementary Fig. 2a, b). Organotypic cultures of wild-type E14.5 brain slices were transduced with GFP-expressing retroviruses to label APs before being treated with submaximal doses of iPLK1. PLK1 inhibition induced a significant increase in the number of BPs, whereas the number of APs that stayed at the ventricular surface decreased (Fig. 2a). A significant increase in BPs was also observed in brain slices taken from Plk1(+/−) embryos, confirming an on-target effect of these inhibitors (Fig. 2a). We next monitored cell fate of GFP-labeled APs by using time-lapse microscopy (Fig. 2b). Plk1(+/−) APs or wild-type progenitors treated with two structurally different iPLK1 displayed a significant increase of cells delaminating from the ventricular surface during a 72-h observation (Fig. 2c). The number of adventricular mitoses was also increased in Plk1(+/−) and iPLK1-treated slices (Fig. 2d), and classification of the diverse number of divisions based on the localization and morphology of mother and daughter cells identified a decrease in proliferative divisions generating APs in favor of differentiative divisions generating BPs or neuroblasts (Fig. 2e).

We next assessed the effect of these inhibitors on neurodevelopment in vivo by injecting submaximal doses to wild-type pregnant females at E12.5 and analyzing the embryos at E14.5. Whereas high doses of iPLK1 resulted in embryonic lethality mimicking Plk1 loss (data not shown), partial inhibition of PLK1 unexpectedly resulted in an expansion of the developing cortex in the radial dimension (Fig. 3a, b and Supplementary Fig. 3a) without causing other obvious aberrations in the rest of the embryo. Whereas this phenotype did not correlate with expansion of the SOX2 + layer of cells or the orientation of the division plane in apical progenitors (Supplementary Fig. 3b), the increase in cortical thickness was accompanied by an expansion of TBR2 + BPs, which frequently showed mitotic figures in the SVZ (Fig. 3a, c). In addition, defective PLK1 activity resulted in an increased abundance of SOX2/TBR2 double-positive NPs in the VZ of these neocortices, suggesting a premature cell-fate switch from AP to BP cell identity consistent with the expansion of the BP pool during mid-gestation (Supplementary Fig. 3a). Cortical expansion in the radial dimension relies on the activity of BPs [25]. It thus seems that the increase of the cortical thickness present in these iPLK1-treated embryos is likely to be due to an increased activity of BPs in the murine developing neocortex promoted by decreased PLK1 activity.

Interestingly, these observations correlated with significant defects in the maturation of the mother centrosome in apical progenitors. Centrosomes in apical progenitors are known to display an asymmetric maturation with stronger accumulation of pericentriolar material (e.g., γ-tubulin) in the mother centrosome (ODF2-positive), which is typically situated apically during mitosis in APs [7, 8]. This asymmetry, however, was lost in iPLK1-treated samples (Fig. 3d) and greatly diminished in the mutant Plk1(+/−) developing cortex (Supplementary Fig. 3c), mostly due to deficient maturation of the mother centrosome. All these data suggest that defective PLK1 activity promotes differentiative divisions in the developing murine neocortex in the absence of the proper asymmetry that characterizes AP centrosomes during mitosis, leading to a premature radial expansion of the neocortex during mid-gestation.

Microcephaly and altered centrosomal asymmetry in Cdk5rap2- and Cep135-deficient mice
We next compared the phenotype observed upon PLK1 deregulation with that resulting from centrosome alteration in microcephaly (MCPH). To this end, we analyzed the effect of
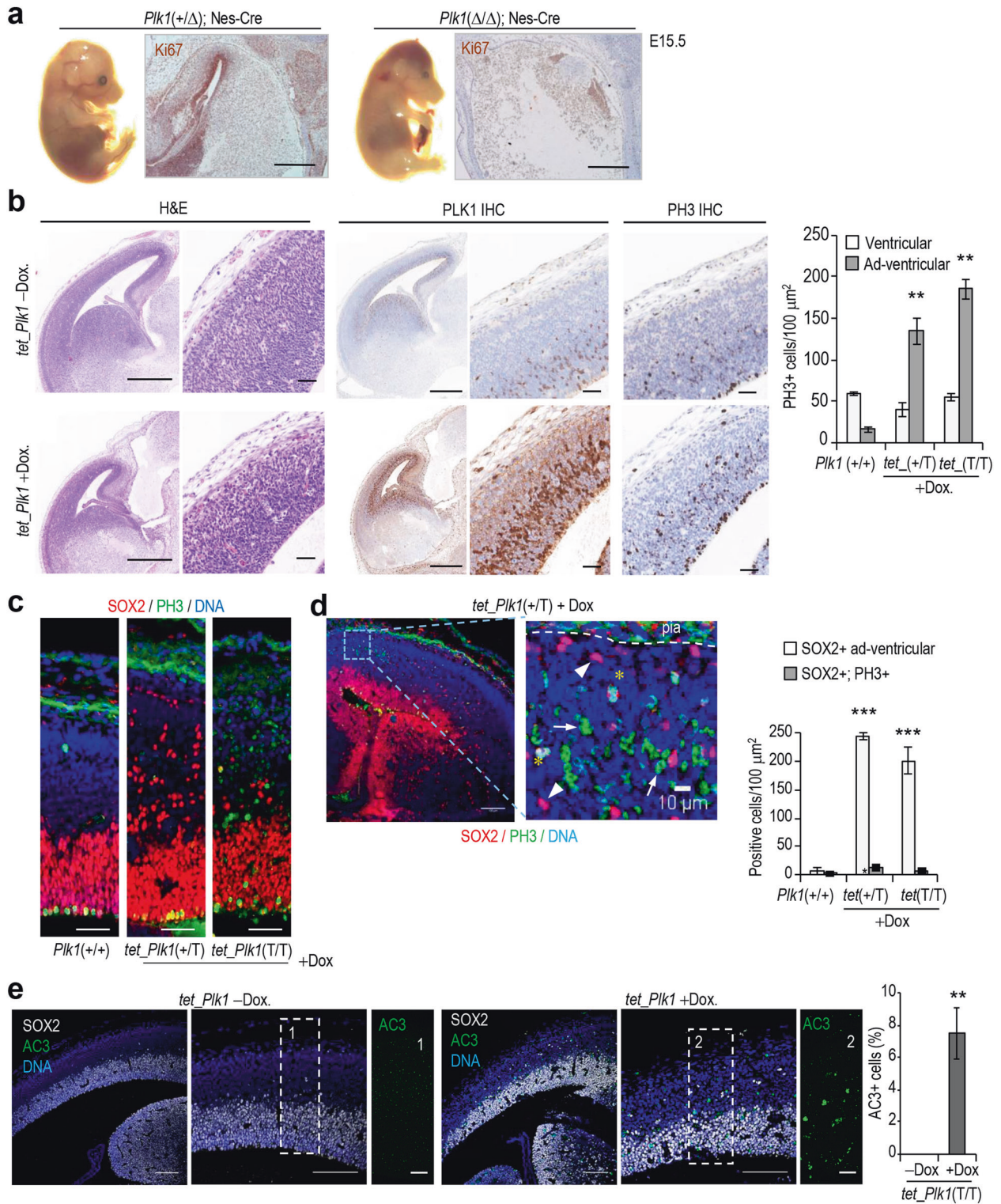
eliminating two different microcephaly genes, *Cdk5rap2* (MCPH3, OMIM #604804) and *Cep135* (MCPH8, OMIM #614673), encoding proteins involved in centrosome structure and dynamics, and centriole assembly and duplication, respectively (Supplementary Fig. 1a). Elimination of *Cdk5rap2* using CRISPR/Cas9 technology [26] promoted dwarfism and microcephaly in mice (Fig. 4a, b and Supplementary Fig. 4a, b). These phenotypes were obvious at birth and progressed within the first month of life (Fig. 4b, c and Supplementary Fig. 4b, c), and were accompanied by

accumulation of aberrations during mitosis in NPs at embryonic day (E) 14.5, mostly represented by monopolar spindles in dividing progenitors of the developing neocortex (Fig. 4d).

Since TP53 is a known mediator of NP cell apoptosis in several MPCH models [26–28], we interbred these mutant mice with a *Trp53*-deficient mouse model to prevent premature NP cell death. *Cdk5rap2*(−/−); *Trp53*(+/−) embryos displayed further accumulation of cellular aberrations with a significant increase of acentrosomal spindles in addition to monopolar figures (Fig. 4d).

Fig. 1 PLK1 deregulation promotes microcephaly in mouse embryos. a Macroscopic images of E15.5 mouse embryos with the indicated *Plk1* genotypes in the presence of a Nestin-Cre recombinase driver. Corresponding micrographs to the right depict immunohistochemical staining for the proliferation marker KI67 (brown) in the developing brain of the same mouse embryos. Scale, 500 μm. **b** Hematoxylin and eosin (H&E) staining, and immunodetection of PLK1 and phosphorylated histone H3 (S10ph; PH3) in histological sections from E14.5 mouse embryos with two copies of the PLK1-inducible construct in the absence or presence of doxycycline (Dox) from E12.5 to E14.5. Scale, 500 μm (lower magnification panels), 50 μm (high-magnification panels). The quantification of PH3 + cells per area unit is shown in the bar plot, including samples with one allele [*tet_Plk1*(+/T)] or two alleles [*tet_Plk1*(T/T)] of the *Plk1*-inducible construct. **c** Confocal imaging of E14.5 mouse brain neocortices of the indicated genotypes stained with antibodies against SOX2 or TBR2. Scale: 100 μm. **d** Confocal micrograph of a cortical area of a *Plk1*-overexpressing E14.5 neocortex and higher-magnification image (right) showing SOX2-positive (arrowheads) and PH3-positive (arrows) cells scattered in the upper layers. Asterisks indicate double SOX2 + ; PH3 + positive cells. Scale 100 μm (left), 10 μm (right). The bar plot to the right shows the quantification of SOX2- and PH3-positive cells from neocortices represented in **c, d**. **e** Confocal imaging of E14.5 mouse neocortices of the indicated genotypes immunostained for SOX2 (gray), active caspase 3 (AC3, green), and staining with DAPI (blue). Dashed and numbered vertical rectangles delimitate cortical areas represented to the right (AC3, green). Scale, 100 μm (left and middle), 25 μm (insets). The bar plot represents a quantification of AC3-positive cells in these neocortices. Data in **b, d, e** represent mean ± SEM from 3 different mice or embryos; **P < 0.01; ***P < 0.001; Student's t-test.

These phenotypes were accompanied by a significant defect in centrosome maturation as scored by γ-tubulin staining, both in the *Cdk5rap2*(−/−); *Trp53*(+/+) and *Cdk5rap2*(−/−); *Trp53*(+/−) models (Fig. 4e). In addition, deficient centrosomal loading of γ-tubulin generated a higher degree of asymmetry in the distribution of this centrosomal maker in the bipolar mitoses observed in mutant NPs (Fig. 4f). Complete elimination of TP53 in a *Cdk5rap2*-null background ultimately resulted in embryonic lethality, with all embryos being resorbed before E11.5, preventing mid-gestation or postnatal studies.

We confirmed these observations in a recent model of MCPH8 with loss-of-function mutations in *Cep135* [26]. Lack of *Cep135* in the presence or absence of TP53 also resulted in microcephaly, accompanied by frequent monopolar and acentrosomal spindles, as well as deficient and asymmetric loading of γ-tubulin onto centrosomes (Fig. 4e–f and Supplementary Fig. 4d). Taken together, these data suggest that loss of function of some MCPH genes can alter the loading of pericentriolar material, leading to a higher degree of asymmetry in their distribution in the centrosome.

Genetic interactions between *Plk1* and microcephaly genes
Given the relevance of PLK1 activity in centrosome regulation by microcephaly genes (Supplementary Fig. 1a), and the opposite effect of partial PLK1 inhibition and MCPH elimination in centrosome asymmetry and cortical growth, we interbred *Plk1*(+/−) and *Cdk5rap2*- or *Cep135*-mutant mice. Elimination of one *Plk1* allele in *Cdk5rap2*(−/−) or *Cep135*(−/−) backgrounds induced stronger microcephaly as scored by the quantification of cortical area (Fig. 5a), head or head/body weight ratios in newborns (Supplementary Fig. 5a, b), or cortical thickness in mid-gestation embryos (Fig. 5b and Supplementary Fig. 5c–e). *Cdk5rap2* or *Cep135* loss-of-function alleles alone or in combination with partial ablation of *Plk1* also generated structurally aberrant embryonic brains presenting critically small neocortices with reduced neurogenesis as scored by significantly reduced TUJ1 + neuroblast layers, occasionally devoid of choroid plexuses and presenting reduced, aberrantly shaped ventricles (Fig. 5b, Supplementary Fig. 5c). In line with these findings, CT scans in adult mice revealed that genetic interaction between *Cdk5rap2* and *Plk1* generated a microcephaly phenotype. These mice presented a strongly reduced skull volume and flat skull, and occasionally hydrocephaly (2 out of 14 P30 mice), likely induced by the choroid-plexus aberrations abovementioned as a result of an impaired cell division of NPs and subsequent aberrant growth of the neocortex (Supplementary Fig. 5f). In addition, we observed a significant cooperation between *Cdk5rap2* and *Plk1* mutations in the induction of TP53 in developing neocortices and the number of apoptotic cells in the VZ of mid-gestation embryos (Fig. 5c). This finding supports the idea that cell death of APs affects more severely the neocortical length or area rather than the thickness

(Supplementary Fig. 5c–e), as growth in the lateral dimension of the neocortex during neurodevelopment relies on the increasing AP cell number derived from the proliferative cell divisions of APs.

At the cellular level, partial ablation of *Plk1* in a microcephaly background resulted in decreased loading of γ-tubulin onto centrosomes (Fig. 6a, b), significant increase in mitotic cells with acentrosomal spindles or disperse γ-tubulin patches not properly loaded onto the centrosomes (Supplementary Fig. 6a), and increased number of cycling neural progenitors with defective centrosome duplication (Fig. 6c). Interestingly, elimination of one allele of *Plk1*, or submaximal inhibition of PLK1, partially corrected the increased asymmetry of γ-tubulin or the mother centriole protein ODF2 induced by *Cdk5rap2* deficiency in NPs in vivo (Fig. 6d, e). However, despite these differences, modulation of PLK1 levels in MCPH-deficient genetic backgrounds was not able to rescue the microcephaly phenotype during neurodevelopment due to the increase in acentrosomal spindles or deficient loading of pericentriolar material to the centrosomes (Supplementary Fig. 6a, b), as well as increased apoptotic cell death (Supplementary Fig. 6c). Whether the increased apoptosis is a consequence of mitotic catastrophe derived from mitotic aberrations or a specific role of PLK1 in inhibiting caspase-dependent cell death [29] is unclear. Taken together, these results highlight the importance of the interplay between structural (CDK5RAP2) and regulatory (PLK1) components of the centrosome in maintaining centrosome asymmetry and genomic stability during neural development, thus preventing developmental diseases such as microcephaly.

DISCUSSION
The frequency of MCPH mutations affecting genes that encode centrosomal proteins suggests an especial sensitivity of neural progenitors for alterations in the centrosomal machinery or the establishment of proper bipolar spindles during mitosis [7]. Several hypotheses have been proposed to explain this sensitivity, including TP53-dependent elimination of genomically unstable cells. *Trp53* ablation rescues apoptotic cell death of neural progenitors with mutations in MCPH genes, but in some cases, it does not rescue microcephaly [26].

An interesting hypothesis suggests that asymmetric cell division is the default division mode in NPs at least partially due to the natural asymmetry in the centrosomal division cycle [7]. After centriole duplication during the S phase, the two centrioles differ in age and maturity, with the mother centriole being loaded with additional structural components that determine specific questions not shared by the newly generated daughter centriole [30, 31]. During neuroepithelial cell division, small changes in spindle orientation can determine whether the cleavage plane bisects or bypasses the small apical domain of dividing neural progenitors and hence determine the outcome of the division. In particular, progenitors retaining the old mother centriole can
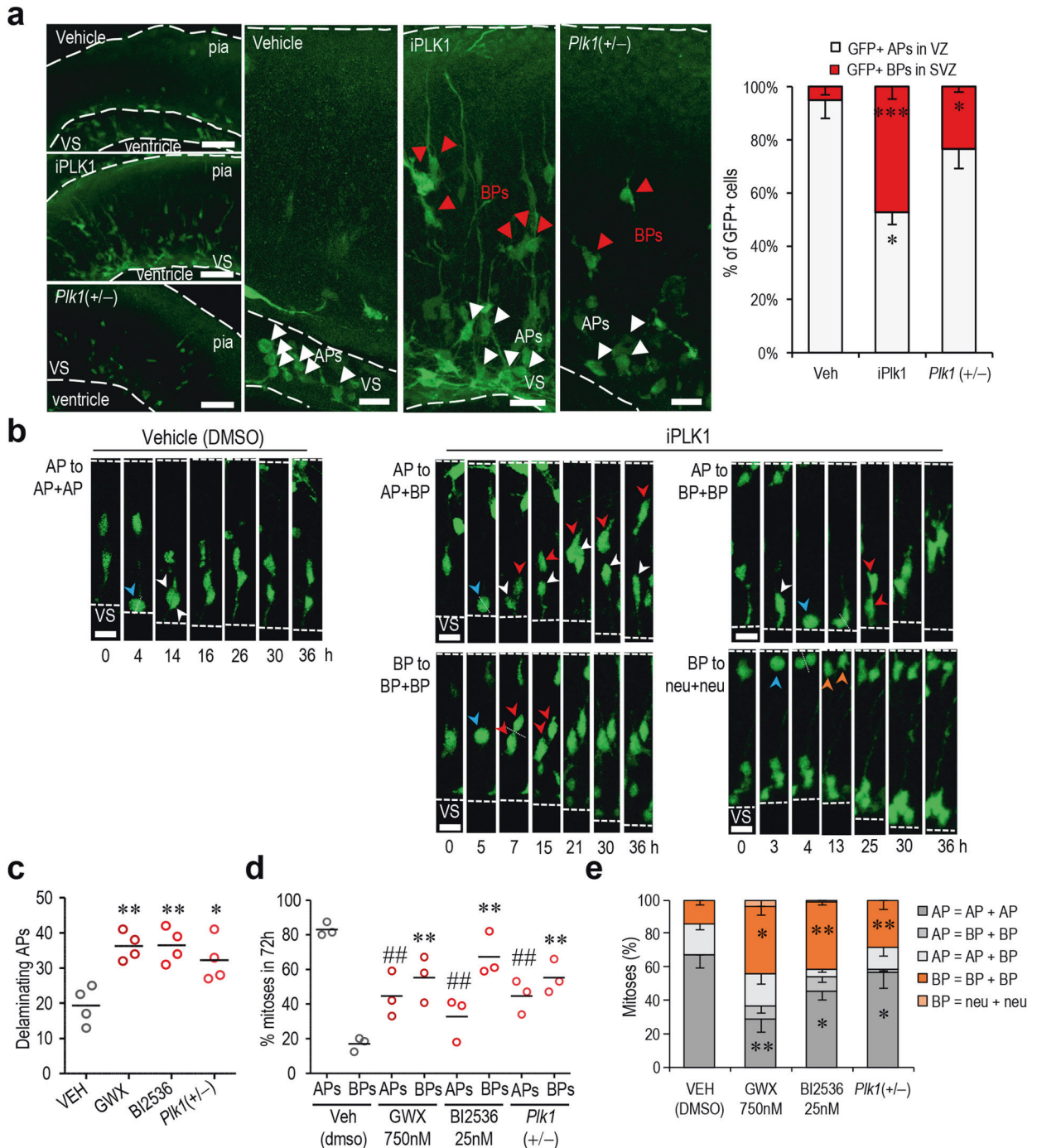
Fig. 2 PLK1 orchestrates progenitor-division mode and cell fate during neurodevelopment. a Confocal imaging of E14.5 brain slices infected with GFP retroviruses targeting apical progenitors for 24 h ex vivo, derived from embryos from *Plk1*(+/−) or wild-type embryos treated with the PLK1 inhibitor GW843682X (iPLK1) ex vivo. White arrowheads, apical progenitors (APs); red arrowheads, basal progenitors (BPs). VS: ventricular surface; pia: piamater. Scale: 100 μm (slices), 25 μm (higher magnification insets). The bar plot shows the quantification of the different GFP+ cell populations. **b** Representative examples of confocal time-lapse imaging of live ex vivo brain slices of E14.5 neocortices treated with vehicle (DMSO) or iPLK1 during the indicated time frames. Each panel of time-lapse insets represents a distinct mode of NP division. Blue arrowheads indicate mitoses, white arrowheads indicate APs (GFP+ cells dividing in VS), red arrowheads indicate BPs (GFP+ cells dividing in SVZ). Scale: 15 μm. **c** Quantification of delaminating GFP+ cells represented in **b**. **d** Quantification of the percentage of mitoses from APs and IPs in 72 h in the indicated neocortices. **e**, Quantification of mitoses in slices from **b** as scored by the resulting cell fate. In **c** and **d** each individual data point represents one slice of the medial aspect neocortex from a different E14.5 embryo. Data represent mean ± SEM from 3 different embryos. ns nonsignificant; *P < 0.05; **P < 0.01; ***P < 0.001; 1-way ANOVA test with Tukey's multiple-comparison test. In **d**, # indicates the statistical comparison between the IP group of each experimental group vs. vehicle.
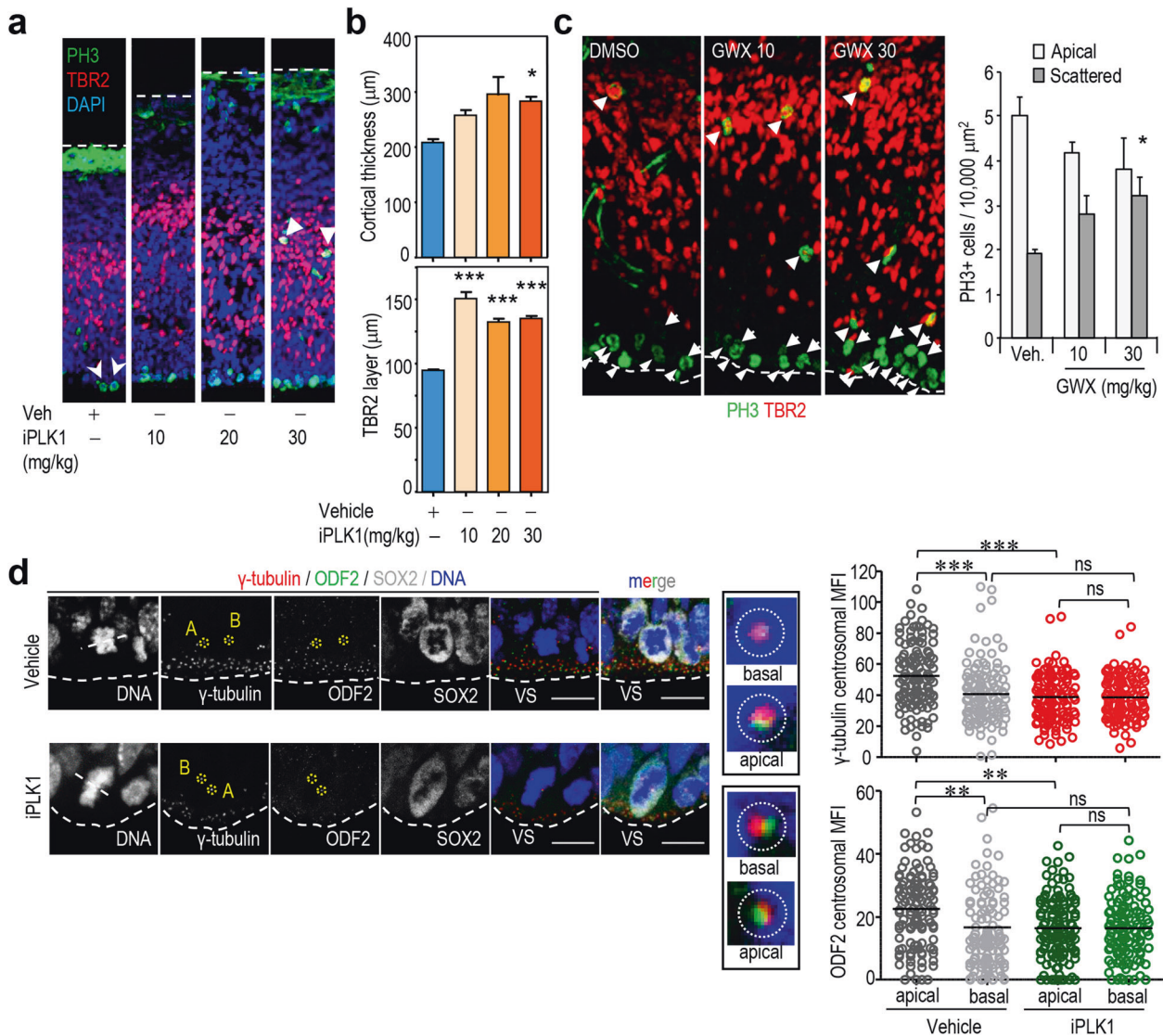
Fig. 3 Deficient PLK1 activity alters cortical neurodevelopment in mouse embryos. a Representative confocal imaging of wild-type E14.5 cortices from equivalent neuroanatomical regions in the medial aspect of the developing brain immunostained with the indicated antibodies. Embryos were treated during mid-gestation (E12.5) with vehicle (DMSO) or the PLK1 inhibitor GW843682X (iPLK1) at the submaximal dosages indicated. Open and closed arrowheads indicate ventricular or adventricular mitoses, respectively. **b** Quantification of cortical thickness (upper) and thickness of the TBR2+ layer of progenitors (lower) in embryos shown in **a**. **c** Detailed immunofluorescence staining of E14.5 neocortices treated with vehicle or GW843682X at the stated doses. Arrowheads and arrows indicate ventricular or adventricular PH3+ mitoses, respectively. The abundance of PH3+ cells in the VZ or SVZ layers is shown to the right. **d** Confocal imaging of E14.5 ventricular NPs immunostained with the indicated antibodies. Embryos were treated with vehicle (DMSO) or 30 mg/Kg GW843682X (iPLK1). Insets to the right display high-magnification micrographs of apical (**A**, proximal to the ventricular surface) and basal (**B**, distal) centrosomes. The quantification was always done at the focal plane of the highest γ-tubulin staining. Scale: 20 μm. The strip plots display the quantification of the centrosomal γ-tubulin mean fluorescence intensity (MFI in arbitrary units) or centrosomal cenexin/ODF2 MFI in these samples. Data represent >100 centrosomes per sample. Data in **b–d** represent mean ± SEM from 3 different mice or embryos; ns nonsignificant; *$P < 0.05$; **$P < 0.01$; ***$P < 0.001$; 1-way ANOVA test with Tukey's multiple-comparison test.

reorganize a new apical polarity complex that determines apical localization and correlates with apical progenitor features [32]. Defects in MCPH genes lead to defective loading of centrosomal components, and our data in *Cdk5rap2-* and *Cep135*-deficient embryos suggest that these mutations correlate with a significant increase in centrosomal asymmetry, a condition suggested to enhance premature neurogenesis likely contributing to micro-cephaly [7].

Although most research has focused on those structural components of centrosomes mutated in MCPH, some evidences suggest that master centrosomal regulatory kinases such as members of the Aurora or Polo families may play a relevant role in cell division and cell fate during neuroepithelial cell division. Aurora A/B phosphorylate the MCPH protein WDR62 (*MCPH2*) and these proteins biochemically and genetically interact to regulate spindle formation, mitotic progression and brain size [33–36]. PLK4, a kinase involved in centriole duplication, has been found mutated in patients with dwarfism and microcephaly [37–39], and its overexpression may lead to microcephaly in the mouse [40].

PLK1, the founding member of the Polo-like kinase family [18], plays multiple roles in centrosome structure and function [19, 20]. PLK1 drives the phosphorylation of both CDK5RAP2 [10] and WDR62 [41] (Supplementary Fig. 1a), and participates in neural development by modulating spindle orientation [42, 43]. Although
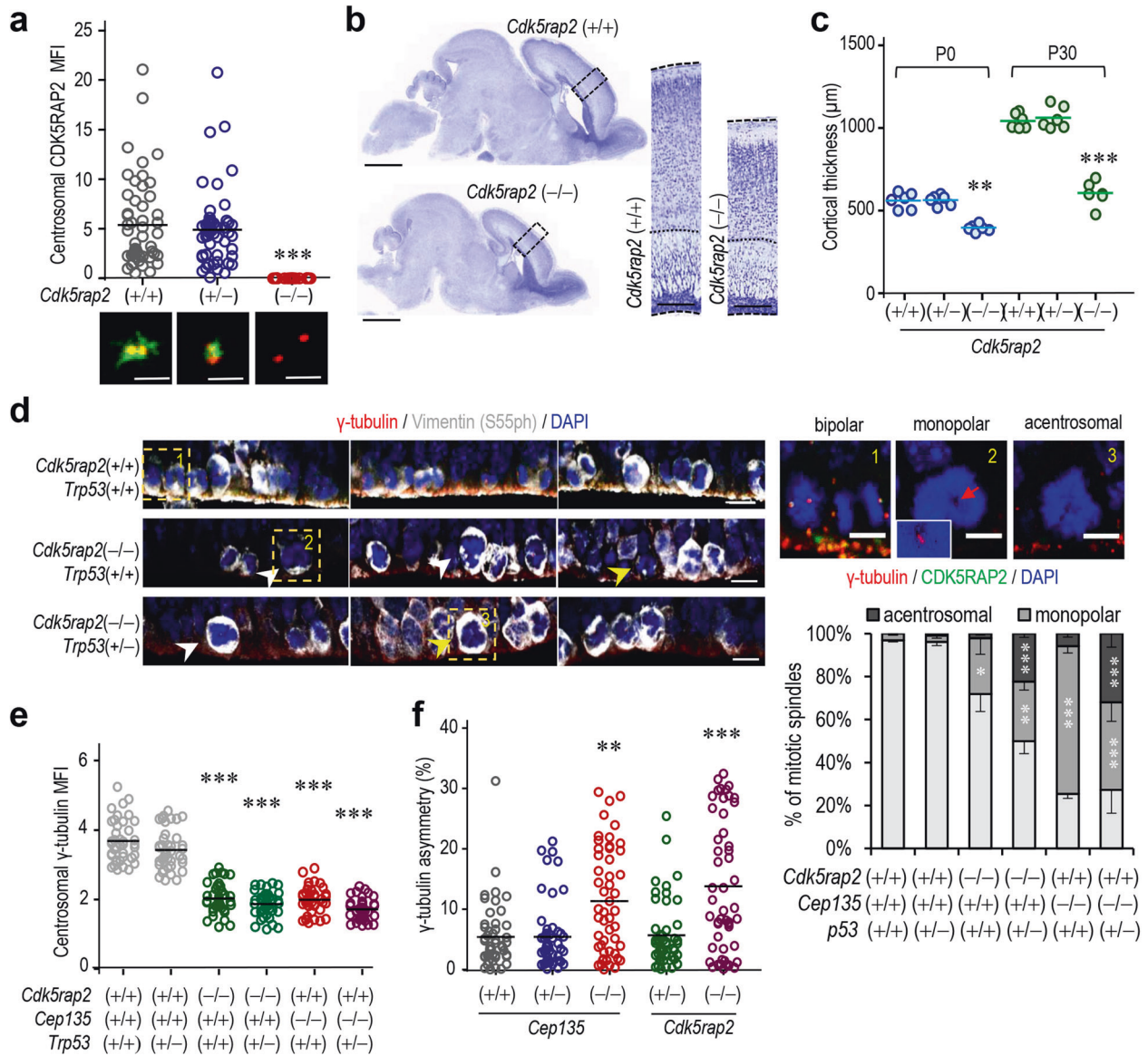
Fig. 4 Centrosomal defects in *Cdk5rap2*- and *Cep135*-deficient mice. a Quantification of CDK5RAP2 centrosomal protein levels (mean fluorescence intensity MFI) in cultured fibroblasts from embryos of the indicated genotypes. Representative confocal micrographs (bottom panels) for each of the genotypes: γ-tubulin (red) and CDK5RAP2 (green). Scale, 1 μm. **b** Nissl staining of sagittal histological sections of P0 newborn brains. Scale: 1 mm (whole-brain sections), 250 μm (insets). The space between dashed and dotted lines in the insets depicts the neocortical area. **c** Cortical thickness of P0 (blue) and P30 (green) brains with the indicated genotypes. **d** Confocal imaging of the innermost ventricular surface neural progenitors of E14.5-developing mouse brains from the indicated genotypes immunostained for γ-tubulin (centrosomes) and vimentin (phospho-S55, mitotic cells). White arrowheads indicate monopolar spindles, yellow arrowheads indicate acentrosomal cells. Numbered squared areas correspond to insets depicted to the right. The stacked bar plot shows a quantification of aberrations in mitotic cells. Scale, 25 μm (left), 10 μm (insets). **e** Quantification of the mean fluorescence intensity of centrosomal γ-tubulin from the cells depicted in **c**. **f** Quantification of the percentage of asymmetry (scored as the difference in intensity between the mother and daughter centrosome in arbitrary units) for centrosomal γ-tubulin in cells from **d**. Data in **b**–**f** represent mean ± SEM from 3 different mice or embryos; ns nonsignificant; *$P < 0.05$; **$P < 0.01$; ***$P < 0.001$ (1-way ANOVA test with Tukey's multiple comparison test).

no mutations in *PLK1* have been found in MCPH patients, *PLK1* maps to 16p12.1 within a region in human chromosome 16 (16p11.2–p12.2) that contains multiple copy number variation hotspots leading to several microdeletions and duplications [11]. Patients with microdeletions/duplications in this region display a variety of defects, including developmental delay, dysmorphic features, including both micro and macrocephaly, and neuropsychiatric disorders [15]. The complexity of these genomic alterations and the number of genes involved makes it difficult to establish specific gene–phenotype correlations. Our data using PLK1-overexpressing mice suggest that increased PLK1 activity

may lead to developmental defects and microcephaly. On the other hand, deletion of a single *Plk1* allele does not induce major obvious defects in the mouse, although significantly cooperates with other alterations such as mutations in MCPH genes.

Among all the different phenotypes induced by PLK1 inhibition in utero, we observed a significant increase in thickness of the developing cortex, accompanied by expansion of progenitors to the adventricular layers of the neuroepithelium, a phenotype that contrasted with the microcephaly observed in MCPH models. In addition, whereas *Cdk5rap2*- and *Cep135*-deficient progenitors displayed increased centrosomal asymmetry, PLK1 inhibition
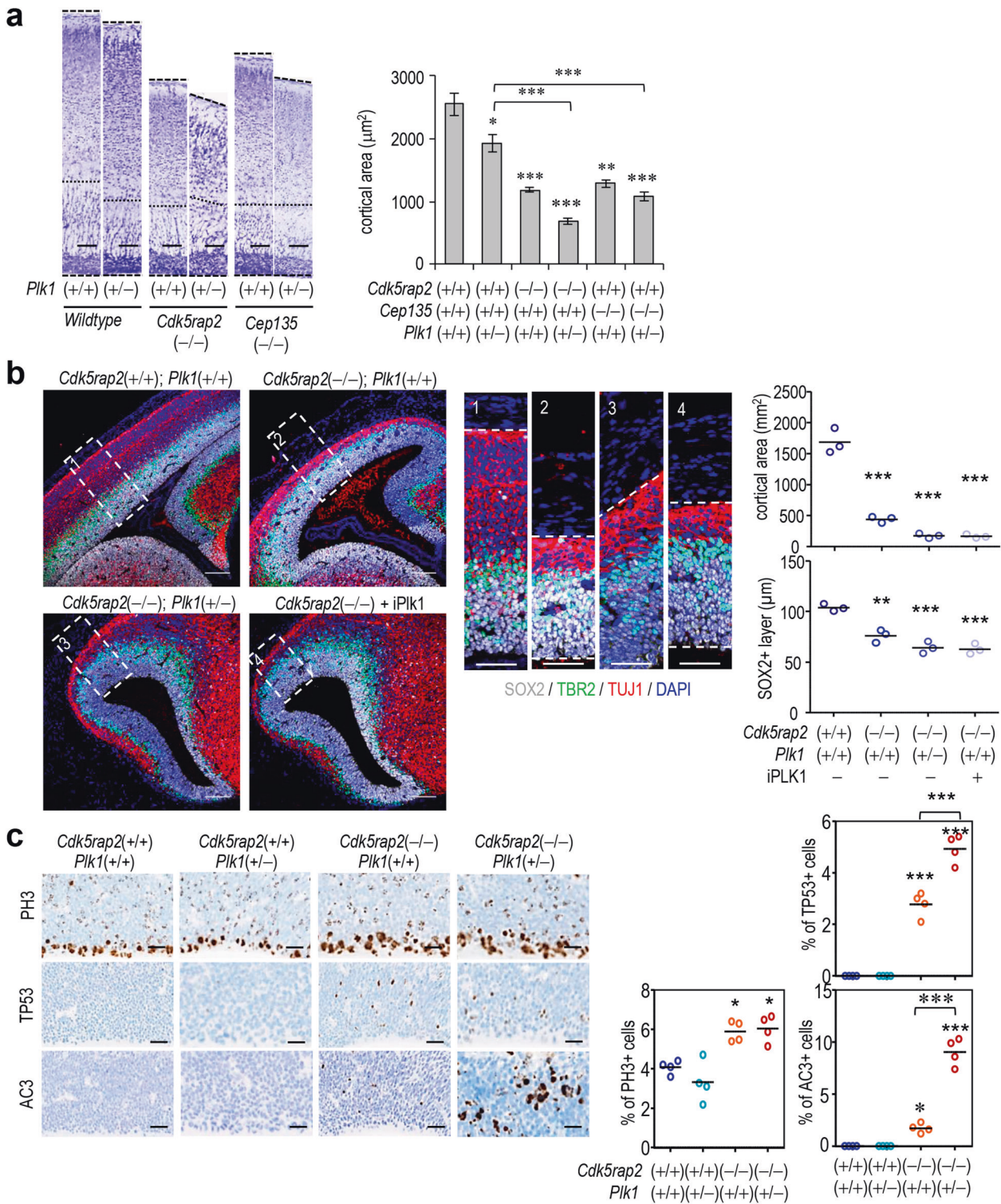
Fig. 5 **Cdk5rap2 and Plk1 genetically interact to induce microcephaly in mice. a** Histological Nissl staining of P0 brains from mouse newborns from the indicated genotypes. Scale: 50 μm. The bar plot shows the quantification of the cortical thickness from the brains depicted in **a**. **b** Confocal imaging of coronal sections from E14.5 neocortices from the indicated genotypes, immunostained with the stated antibodies. Note the aberrant shape of the neocortex and the absence of choroid plexuses upon PLK1 modulation. Numbered cortical regions correspond to insets to the right. Scale: 100 μm. The plots depict the quantification of cortical area (upper) or the SOX2+-layer thickness in these samples. **c** Immunohistochemical staining of the ventricular zone from E14.5 embryos from the stated genotypes with the indicated antibodies (brown). Scale: 100 μm. The plots indicate the quantification of PH3 + , p53 + , or active caspase-3 (AC3) + cells in these samples. Data in **b**, **c**, represent mean ± SEM from 3 different embryos; ns nonsignificant; *$P < 0.05$; **$P < 0.01$; ***$P < 0.001$; 1-way ANOVA test with Tukey's multiple-comparison test.
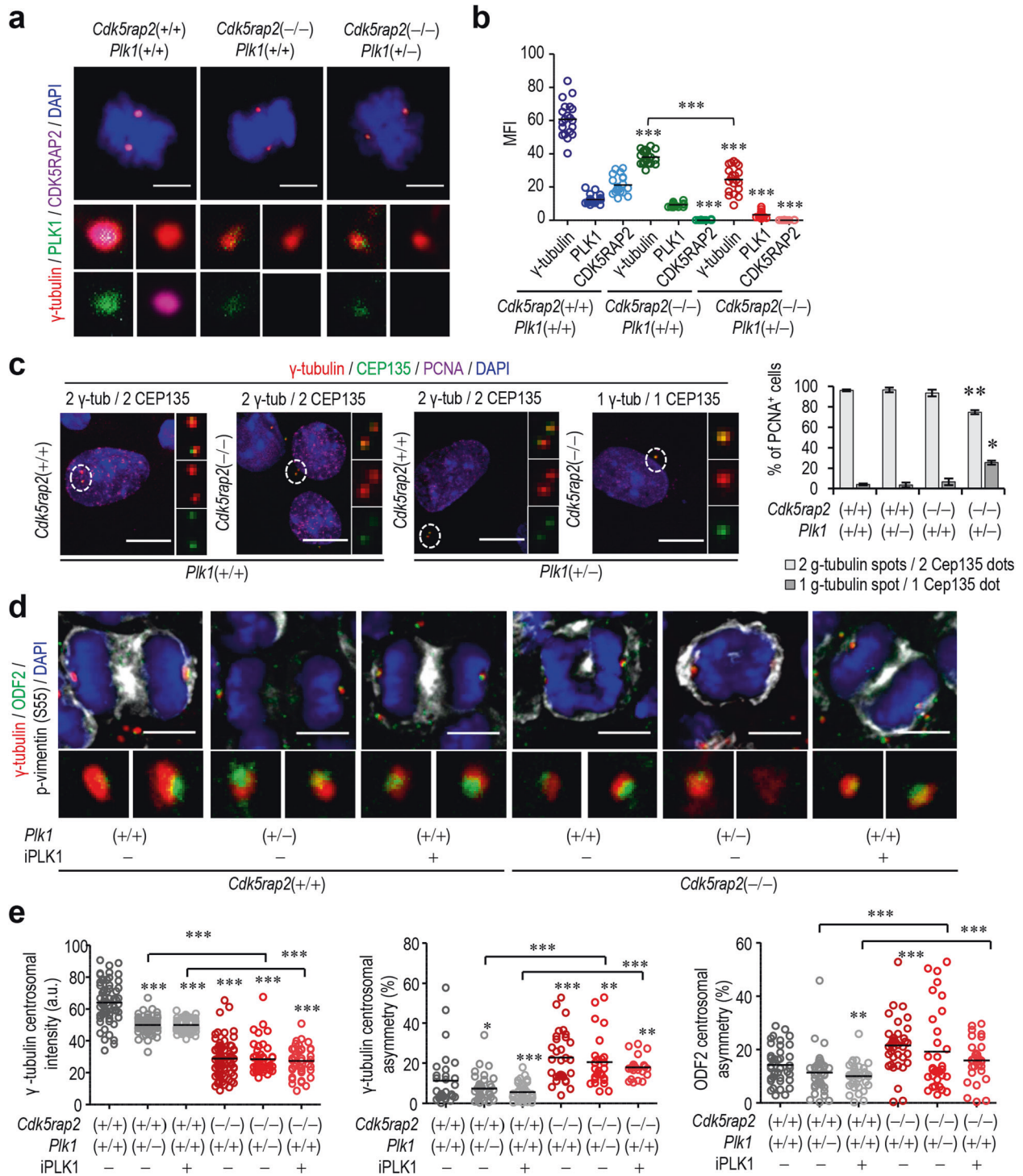
J. González-Martínez et al.

Fig. 6 PLK1 and CDK5RAP2 display opposite forces in the control of centrosome asymmetry. a Confocal micrographs of immunofluorescence staining from E14.5 primary MEFs of the indicated genotypes with the stated antibodies against centrosomal proteins. Scale: 10 μm. **b** Quantification of the mean fluorescence intensity (MFI) in arbitrary units of the centrosomal proteins displayed in **a**. The asterisks refer to the comparison with double wild-type samples, unless indicated otherwise. **c** Confocal micrographs of primary MEFs from the indicated genotypes immunostained with the stated antibodies. The plots indicate the quantification of the percentage of PCNA + cells with different combinations of γ-tubulin and CEP135 signals. **d** Immunodetection of γ-tubulin and ODF2 in APs lining the ventricular surface of E14.5 mouse embryos of the indicated genotypes. Scale: 5 μm. **e** Quantification of centrosomal γ-tubulin intensity (left) and asymmetry (middle) and cenexin/ODF2 asymmetry (right) in arbitrary units. The asterisks refer to the comparison with untreated double wild-type samples, unless indicated otherwise. Data in **b, c, e** represent cells from 3 different embryos; *$P < 0.05$; **$P < 0.01$; ***$P < 0.001$; 1-way ANOVA test with Tukey's multiple-comparison test.

resulted in decreased asymmetry and slightly limited the asymmetry observed in the MCPH models. Although we are aware that our data do not show a causal effect between the changes in centrosomal asymmetry and brain growth, these data suggest that changes in *PLK1* copy number, as the ones observed in the 16p11.2–p12.2 microdeletion and microduplication syndromes, or in PLK1 activity, may contribute to a variety of developmental defects and may also modulate centrosomal defects associated with microcephaly.

MATERIALS AND METHODS
Generation of mutant mice
Germline or conditional *Plk1*-deficient [21, 22, 44] and -overexpressing [23] mice were reported previously. The *Cdk5rap2*- and *Cep135*-deficient mice have been reported recently [26]. *Trp53*-knockout and Nestin-Cre mice were obtained from Jackson Laboratories (B6.129S2-Trp53tm1Tyj/J; JAX stock #002101; and B6.Cg-Tg(Nes-cre)1Kln/J; JAX stock # 003771, respectively). Mice were maintained on a C57BL/6J-129 mixed genetic background and were housed in a pathogen-free animal facility at the CNIO following the animal care standards of the institution. All animal protocols were approved by the Instituto de Salud Carlos III. For histological examination of paraffin samples, samples were fixed in a solution of 4% paraformaldehyde, and embedded in paraffin. About 2.5–5-micrometer-thick sections were stained with hematoxylin and eosin, Nissl, or cresyl-violet staining protocols.

Immunofluorescence of cryosections
For histological analysis of cryosections, whole mid-gestation embryos or sectioned embryonic heads were dissected and fixed in 4% paraformaldehyde (PFA) in PBS (0.1 M phosphate buffer, pH 7.3), cryoprotected overnight in 30% sucrose (dissolved in water), frozen in Tissue-Tek OCT, and cryosectioned at 14 μm by a cryostat (Microm). Primary antibodies were applied in the sections in the indicated concentrations (Supplementary Table 1) and incubated overnight at 4 °C in a humid chamber. The corresponding secondary antibodies (Molecular Probes Alexa Fluor dyes) were used at a concentration of 1:500 and incubated at room temperature during 3 h, followed by three washing steps of 5 min and one staining incubation of 15 min with 4′,6-diamidino-2-phenylindole (DAPI, to stain nuclei) when indicated. Sections were covered with fluoromount mounting medium and visualized in a Leica TCS SP5 confocal microscope using a HCX PLAN APO CS 63x/1.4 Oil Immersion, HCX PLAN APO CS 40×/1.4 Oil Immersion, or HCX PLAN APO CS 20×/1.4 objective.

For in vitro studies, NPs or MEFs were grown onto glass coverslips and fixed in PFA 4% for 10 min at room temperature or ice-cold methanol for 5 min at −20 °C (when indicated, for centriolar proteins) and then washed three times in PBS, blocked in 3% normal horse serum (Vector Biolabs), and incubated in blocking solution with the primary antibodies included in Supplementary Table 1. The rest of the steps were similar to those followed for cryosections.

Immunohistochemistry
Embryos or tissues were fixed in 10% buffered formalin stabilized with methanol (Sigma) and embedded in paraffin blocks for histological analysis. Immunohistochemistry was performed on 2.5-μm paraffin sections by using an automated protocol developed for the DISCOVERYXT-automated slide-staining system (Ventana Medical Systems Inc.). All steps were performed in this staining platform by using validated reagents, including deparaffinization, antigen retrieval with sodium citrate buffer, antibody incubation, and detection. Primary antibodies used in this study are listed in Supplementary Table 1. Appropriate biotinylated secondary antibodies were used to detect the primary antibodies before mentioned, followed by incubation with streptavidin–horseradish peroxidase and a diaminobenzidine system. Full slides were digitalized with a Zeiss AxioScan Z1, and analyzed by using the ZEISS Zen 2.3 Imaging Software (Zeiss).

Molecular imaging
Computerized axial tomography scanning (CT scan) was performed on anesthetized P30 mice [3% of Isoflurane (Isoba Vet)] using an eXplore ista PET-CTscan (GE Healthcare) with the following parameters: 200 mA, 35 kV, 160 m, 16 shots, and 360 projections. MMWKS (GE Healthcare) and MicroView software were used to analyze the resulting images.

MEF in vitro culture
For in vitro studies, E14.5 embryos were dissected, heads were cut off and discarded as well as the embryonic liver. The remaining embryonic tissue was mechanically dissociated first and trypsinized. MEFs obtained afterward were cultured in DMEM with 10% of FBS and gentamycin. For all experiments in this work, passage-0 (P0) MEFs were used.

Primary NP isolation and in vitro culture
Primary neural progenitors (NPs) were obtained from E14.5 embryos. Briefly, E14.5 embryonic forebrains were dissected under aseptic conditions; neocortices from dorsal telencephalon were separated and digested with papain (Worthington #LS00310). Papain was activated in a home-made activation solution consisting of 5.5 mM L-cysteine (Sigma, #C8277) and 1.1 mM EDTA (Sigma, #E6511) in EBSS (Gibco #24010-043) following the manufacturer's instructions, filtered through a 0.22 μM filter, and used at a concentration of 12 U/ml (1 ml/two hemicortices) together with DNAse I (Gibco) for 30 min at 37 °C. NPs obtained were pelleted in DMEM/Hams F-12 (Gibco) and activation solution removed completely. NPs were cultured in suspension in a medium containing DMEM/Hams F-12 (Gibco #11320033), 5 mM hepes, 1 mM sodium pyruvate, 2 mM L-glutamine, N2 supplement (Gibco #17502048), B27 supplement (Gibco #17504044), 0.7 U/ml heparin sodium salt (Sigma #H3149), 20 ng/ml mouse EGF (Gibco #PMG8044), 20 ng/ml mouse FGF2 (Gibco #PMG0034), and penicillin/streptomycin (Gibco #15140148). When needed, neurospheres were dissociated with Accutase (Gibco) for 5 min at 37 °C prior to experiment plating.

Ex vivo culture of brain slices and time-lapse videomicroscopy
For brain-slice preparation, E14.5 embryonic brains were dissected out and kept in 4 °C HBSS supplemented with Ca2 + , Mg, and sucrose. Embryonic brains were then embedded squared, plastic cryomolds filled with low-melting agarose warmed to 38 °C, and positioned in a rostrocaudal orientation. Agarose-embedded brains were then kept on ice, until agarose was solid, and cut in a Leica VT-1000S vibratome in 250-μm-thick slices with the following settings: speed 4, frequency 5. All the experimental procedure were carried out in maximum 1 h at 4 °C. Brain slices were cultured in a medium containing DMEM/F12 medium, 5% FBS (Gibco), normal horse serum (NHS, Gibco) 5%, N2 supplement (Gibco, 1:100), B-27 supplement (Gibco, 15:50), sodium bicarbonate (0.3 g/L), glutamine (1%), glucose (0.66%), and Pen/strep as antibiotic [45, 46]. Slices were infected by placing a drop of slice medium containing home-made-produced GFP retroviruses in the ventricle of each slice, and incubating the slice for 24 h with the viral supernatant. About 24 h later, slices were immobilized in 8-well IBIDI chambers with glass bottom in a collagen solution (375 μl of collagen Ia, 365 μl of slice medium, and 9.4 μL of NaOH 1 M) [45]. Brain slices were then covered with slice medium containing the indicated small-molecule inhibitors in each case, and analyzed in a Leica TCS SP5 confocal microscope using a HCX PLAN APO CS 20×/1.4 objective, with a 2–4 confocal zoom factor. Confocal images were taken in time frames of 30 min, 5-μm stacks, avoiding the first and last 50 μm of slice to avoid cell artifacts, for 72 h, marking several positions per slice. Analysis of the resulting time-lapse videos was performed with ImageJ software (Fiji).

Statistical analyses
Statistics was performed using Prism software (GraphPad Software) or Microsoft Excel. Sample size was not predefined and the principles of 3Rs (replacement, reduction and refinement) were considered for animal work. No randomization method was used. Unless stated otherwise, all statistical tests of comparative data were done using a 1-way ANOVA with a Tukey multiple comparison post hoc test in experiments with more than 2 experimental groups, or an unpaired, 2-sided Student's *t*-test with Welch's correction when appropriate. Data are expressed as the mean of at least 3 independent experiments ± SEM, with a *P*-value of less than 0.05 considered statistically significant.

DATA AVAILABILITY
Data sharing not applicable to this article as no datasets were generated or analyzed during the current study.

J. González-Martínez et al.

REFERENCES

1. Bettencourt-Dias M, Glover DM. Centrosome biogenesis and function: centrosomics brings new understanding. Nat Rev Mol Cell Biol. 2007;8:451–63.
2. Wu J, Akhmanova A. Microtubule-Organizing Centers. Annu Rev Cell Dev Biol. 2017;33:51–75.
3. Nigg EA, Holland AJ. Once and only once: mechanisms of centriole duplication and their deregulation in disease. Nat Rev Mol Cell Biol. 2018;19:297–312.
4. Jayaraman D, Bae BI, Walsh CA. The genetics of primary microcephaly. Annu Rev Genomics Hum Genet. 2018;19:177–200.
5. Florio M, Huttner WB. Neural progenitors, neurogenesis and the evolution of the neocortex. Development. 2014;141:2182–94.
6. Taverna E, Gotz M, Huttner WB. The cell biology of neurogenesis: toward an understanding of the development and evolution of the neocortex. Annu Rev Cell Dev Biol. 2014;30:465–502.
7. Saade M, Blanco-Ameijeiras J, Gonzalez-Gobartt E, Marti E. A centrosomal view of CNS growth. Development. 2018;145:21.
8. Wang X, Tsai JW, Imai JH, Lian WN, Vallee RB, Shi SH. Asymmetric centrosome inheritance maintains neural progenitors in the neocortex. Nature. 2009;461:947–55.
9. Barr FA, Sillje HH, Nigg EA. Polo-like kinases and the orchestration of cell division. Nat Rev Mol Cell Biol. 2004;5:429–40.
10. Hanafusa H, Kedashiro S, Tezuka M, Funatsu M, Usami S, Toyoshima F, et al. PLK1-dependent activation of LRRK1 regulates spindle orientation by phosphorylating CDK5RAP2. Nat Cell Biol. 2015;17:1024–35.
11. Ballif BC, Hornor SA, Jenkins E, Madan-Khetarpal S, Surti U, Jackson KE, et al. Discovery of a previously unrecognized microdeletion syndrome of 16p11.2-p12.2. Nat Genet. 2007;39:1071–3.
12. Kumar RA, KaraMohamed S, Sudi J, Conrad DF, Brune C, Badner JA, et al. Recurrent 16p11.2 microdeletions in autism. Hum Mol Genet. 2008;17:628–38.
13. Weiss LA, Shen Y, Korn JM, Arking DE, Miller DT, Fossdal R, et al. Association between microdeletion and microduplication at 16p11.2 and autism. N Engl J Med. 2008;358:667–75.
14. Rosenfeld JA, Coppinger J, Bejjani BA, Girirajan S, Eichler EE, Shaffer LG, et al. Speech delays and behavioral problems are the predominant features in individuals with developmental delays and 16p11.2 microdeletions and microduplications. J Neurodev Disord. 2010;2:26–38.
15. Barber JC, Hall V, Maloney VK, Huang S, Roberts AM, Brady AF, et al. 16p11.2-p12.2 duplication syndrome; a genomic condition differentiated from euchromatic variation of 16p11.2. Eur J Hum Genet. 2013;21:182–9.
16. D'Angelo D, Lebon S, Chen Q, Martin-Brevet S, Snyder LG, Hippolyte L, et al. Defining the effect of the 16p11.2 duplication on cognition, behavior, and medical comorbidities. JAMA Psychiatry. 2016;73:20–30.
17. Niarchou M, Chawner S, Doherty JL, Maillard AM, Jacquemont S, Chung WK, et al. Psychiatric disorders in children with 16p11.2 deletion and duplication. Transl Psychiatry. 2019;9:8.
18. Sunkel CE, Glover DM. polo, a mitotic mutant of Drosophila displaying abnormal spindle poles. J Cell Sci. 1988;89:25–38.
19. Bruinsma W, Raaijmakers JA, Medema RH. Switching Polo-like kinase-1 on and off in time and space. Trends Biochem Sci. 2012;37:534–42.
20. Petronczki M, Lenart P, Peters JM. Polo on the rise-from mitotic entry to cytokinesis with Plk1. Dev Cell. 2008;14:646–59.
21. Trakala M, Partida D, Salazar-Roa M, Maroto M, Wachowicz P, de Carcer G, et al. Activation of the endomitotic spindle assembly checkpoint and thrombocytopenia in Plk1-deficient mice. Blood. 2015;126:1707–14.
22. de Carcer G, Wachowicz P, Martinez-Martinez S, Oller J, Mendez-Barbero N, Escobar B, et al. Plk1 regulates contraction of postmitotic smooth muscle cells and is required for vascular homeostasis. Nat Med. 2017;23:964–74.
23. de Carcer G, Venkateswaran SV, Salgueiro L, El Bakkali A, Somogyi K, Rowald K, et al. Plk1 overexpression induces chromosomal instability and suppresses tumor development. Nat Commun. 2018;9:3012.
24. Gutteridge RE, Ndiaye MA, Liu X, Ahmad N. Plk1 inhibitors in cancer therapy: from laboratory to clinics. Mol Cancer Ther. 2016;15:1427–35.
25. Fish JL, Dehay C, Kennedy H, Huttner WB. Making bigger brains-the evolution of neural-progenitor-cell division. J Cell Sci. 2008;121:2783–93.
26. González-Martínez J, Cwetsch AW, Martínez-Alonso D, López-Sainz LR, Almagro J, Melati A, et al. Deficient Adaptation to Centrosome Duplication Defects in Neural Progenitors Causes Microcephaly and Subcortical Heterotopias. JCI Insights 2021, in press.
27. Marjanovic M, Sanchez-Huertas C, Terre B, Gomez R, Scheel JF, Pacheco S, et al. CEP63 deficiency promotes p53-dependent microcephaly and reveals a role for the centrosome in meiotic recombination. Nat Commun. 2015;6:7676.
28. Phan TP, Maryniak AL, Boatwright CA, Lee J, Atkins A, Tijhuis A, et al. Centrosome defects cause microcephaly by activating the 53BP1-USP28-TP53 mitotic surveillance pathway. EMBO J. 2021;40:e106118.
29. Matthess Y, Raab M, Knecht R, Becker S, Strebhardt K. Sequential Cdk1 and Plk1 phosphorylation of caspase-8 triggers apoptotic cell death during mitosis. Mol Oncol. 2014;8:596–608.
30. Nigg EA, Stearns T. The centrosome cycle: Centriole biogenesis, duplication and inherent asymmetries. Nat Cell Biol. 2011;13:1154–60.
31. Meiring JCM, Shneyer BI, Akhmanova A. Generation and regulation of microtubule network asymmetry to drive cell polarity. Curr Opin Cell Biol. 2020;62:86–95.
32. Das RM, Storey KG. Apical abscission alters cell polarity and dismantles the primary cilium during neurogenesis. Science. 2014;343:200–4.
33. Chen JF, Zhang Y, Wilde J, Hansen KC, Lai F, Niswander L. Microcephaly disease gene Wdr62 regulates mitotic progression of embryonic neural stem cells and brain size. Nat Commun. 2014;5:3885.
34. Sgourdou P, Mishra-Gorur K, Saotome I, Henagariu O, Tuysuz B, Campos C, et al. Disruptions in asymmetric centrosome inheritance and WDR62-Aurora kinase B interactions in primary microcephaly. Sci Rep. 2017;7:43708.
35. Lim NR, Yeap YY, Ang CS, Williamson NA, Bogoyevitch MA, Quinn LM, et al. Aurora A phosphorylation of WD40-repeat protein 62 in mitotic spindle regulation. Cell Cycle. 2016;15:413–24.
36. Huang J, Liang Z, Guan C, Hua S, Jiang K. WDR62 regulates spindle dynamics as an adaptor protein between TPX2/Aurora A and katanin. J Cell Biol. 2021; 220: e202007167.
37. Martin CA, Ahmad I, Klingseisen A, Hussain MS, Bicknell LS, Leitch A, et al. Mutations in PLK4, encoding a master regulator of centriole biogenesis, cause microcephaly, growth failure and retinopathy. Nat Genet. 2014;46:1283–92.
38. Tsutsumi M, Yokoi S, Miya F, Miyata M, Kato M, Okamoto N, et al. Novel compound heterozygous variants in PLK4 identified in a patient with autosomal recessive microcephaly and chorioretinopathy. Eur J Hum Genet. 2016;24:1702–6.
39. Martin-Rivada A, Pozo-Roman J, Guemes M, Ortiz-Cabrera NV, Perez-Jurado LA, Argente J. Primary dwarfism, microcephaly, and chorioretinopathy due to a PLK4 mutation in two siblings. Horm Res Paediatr. 2020;93:567–72.
40. Marthiens V, Rujano MA, Pennetier C, Tessier S, Paul-Gilloteaux P, Basto R. Centrosome amplification causes microcephaly. Nat Cell Biol. 2013;15:731–40.
41. Miyamoto T, Akutsu SN, Fukumitsu A, Morino H, Masatsuna Y, Hosoba K, et al. PLK1-mediated phosphorylation of WDR62/MCPH2 ensures proper mitotic spindle orientation. Hum Mol Genet. 2017;26:4429–40.
42. Sakai D, Dixon J, Dixon MJ, Trainor PA. Mammalian neurogenesis requires Treacle-Plk1 for precise control of spindle orientation, mitotic progression, and maintenance of neural progenitor cells. PLoS Genet. 2012;8:e1002566.
43. Connell M, Chen H, Jiang J, Kuan CW, Fotovati A, Chu TL, et al. HMMR acts in the PLK1-dependent spindle positioning pathway and supports neural development. Elife. 2017; 6: e28672.
44. Wachowicz P, Fernández-Miranda G, Marugán C, Escobar B, De Carcer G. Genetic depletion of Polo-like kinase 1 leads to embryonic lethality due to mitotic aberrancies. Bioessays. 2016;38:S96–S106.
45. Pilaz LJ, Silver DL. Live imaging of mitosis in the developing mouse embryonic cortex. J Vis Exp. 2014; 10.3791/51298.
46. Noctor SC, Martinez-Cerdeno V, Ivic L, Kriegstein AR. Cortical neurons arise in symmetric and asymmetric division zones and migrate through specific phases. Nat Neurosci. 2004;7:136–44.

AUTHOR CONTRIBUTIONS
JGM performed most in vitro and in vivo assays with the help of AWC and JG. PS and GdC generated and contributed to the analysis of Plk1 models. JG and DM participated in the confocal analysis of images. GG and FM participated in the quantitative analysis of skulls. EMP, PS, and GdC contributed to the characterization of the effect of PLK1 inhibitors. MM supervised the project. All authors analyzed data, and JGM and MM wrote the paper with the help of AWC, JG and EMP.

COMPETING INTERESTS

The authors declare no competing interests.

ETHICS STATEMENT

The animals were observed on a daily basis, and sick mice were humanely euthanized in accordance with the Guidelines for Humane End-points for Animals Used in Biomedical Research (Directive 2010/63/EU of the European Parliament and Council and the Recommendation 2007/526/CE of the European Commission). All animal protocols were approved by the Committee for Animal Care and Research of the Instituto de Salud Carlos III and the Comunidad de Madrid (Madrid, Spain).

ADDITIONAL INFORMATION

Supplementary information The online version contains supplementary material available at https://doi.org/10.1038/s41418-022-00937-w.

Correspondence and requests for materials should be addressed to Marcos Malumbres.

Reprints and permission information is available at http://www.nature.com/reprints

Publisher's note Springer Nature remains neutral with regard to jurisdictional claims in published maps and institutional affiliations.